Ellipse-Line-Ellipse source trajectory and its R-line coverage for long-object cone-beam imaging with a C-arm system

Yu Z.[a,c], Noo F.[a], Lauritsch G.[b], Dennerlein F.[b] and Hornegger J.[c]

[a]Department of Radiology, University of Utah, Salt Lake City, USA;
[b]Siemens AG, Healthcare Sector, Forchheim, Germany
[c]Chair of Computer Science 5, University of Erlangen-Nuremberg, Erlangen, Germany

ABSTRACT

Over the last decade, significant progress has been made in terms of treatment of diseases using minimally-invasive procedures. This progress was facilitated through multiple refinements of the imaging capabilities of C-arm systems in the interventional room, and more sophisticated procedures may become feasible by further refining the performance of these systems. Our primary focus is to eliminate two strong limitations of the current circular cone-beam imaging approach: cone-beam artifacts and limited extent of the volume covered in the direction of the patient bed. To solve this problem, we seek a source trajectory that (i) is complete in terms of Tuy's condition, (ii) can be periodically-repeated without discontinuities to allow long-object imaging, (iii) is practical, and (iv) offers full R-line coverage (an R-line is a line that connects any two source positions). A trajectory that satisfies all of our constraint is the Arc-Extended-Line-Arc (AELA) trajectory. Unfortunately, this trajectory does not allow smooth, continuous scanning at reasonable dose. In this work, we propose a new data acquisition geometry: the Ellipse-Line-Ellipse (ELE) trajectory. This geometry satisfies all of our constraints along with the attractive feature that smooth, continuous scanning at reasonable dose is enabled.

Keywords: R-line, source trajectory, Ellipse-Line-Ellipse, cone-beam

1. INTRODUCTION

Over the last decade, significant progress has been made in terms of treatment of diseases using minimally-invasive procedures. This progress was facilitated through multiple refinements of the imaging capabilities of C-arm systems in the interventional room. Many procedures which were unheard of ten years ago are now clinical routine, and more sophisticated procedures may become feasible by further refining the performance of the imaging system. Our primary focus is to eliminate two strong limitations of the current circular cone-beam imaging approach: cone-beam artifacts and limited extent of the volume covered in the direction of the patient bed. To solve this problem, we seek a source trajectory that (i) is complete in terms of Tuy's condition, (ii) can be periodically-repeated without discontinuities to allow smooth long-object imaging, (iii) is practical, and (iv) offers full R-line coverage (an R-line is a line that connects any two source positions). The most important issue regarding practicality is to acknowledge that a reversal in the rotation direction is needed every 360 degrees due to the mechanical restrictions of C-arm systems. The constraint on R-line coverage is the result of current knowledge on cone-beam tomographic reconstruction: theoretically-exact and stable reconstruction[1–3] is known to be feasible from truncated data when every point within the field-of-view belongs to an R-line; when R-lines are missing, there is no guarantee that accurate reconstruction may be achievable. A trajectory that satisfies all of our constraints is the Arc-Extended-Line-Arc (AELA) trajectory.[4] Unfortunately, this trajectory does not allow smooth, continuous scanning at reasonable dose.

In this work, we propose a new data acquisition geometry: the Ellipse-Line-Ellipse (ELE) trajectory. This geometry satisfies all of our constraints along with the attractive feature that smooth, continuous scanning at reasonable dose is enabled. Identification of the R-line coverage offered by the ELE trajectory is however not trivial. Most of this four-page summary focusses on analyzing this coverage and demonstrating that suitable parameters may be found so as to cover any typical region-of-interest. Note that proofs have been found for all statements made in the summary, but these are not given due to the limited space.

2. GEOMETRY AND NOTATION

The ELE trajectory lies on the surface, $\mathcal{S}$, of a circular cylinder with radius R. It consists of two elliptical arcs and one line, which we refer to as T-arcs and T-line, see Figure 1 (left). Both T-arcs are centered on the symmetry axis of $\mathcal{S}$, which we call the z-axis. The T-arcs can be viewed as the intersections of two planes with $\mathcal{S}$. Those two planes are orthogonal to the (x, z)-plane and intersect in the (x, y)-plane along the line of equation: $x = c$ with $c < -R$. Note that the endpoints of the upper T-arc are denoted as A^i_+ and A^e_+, whereas the endpoints of the lower T-arc are A^i_- and A^e_-. Any point on the upper and lower T-arcs, A^m_+ and A^n_-, can be identified by a polar angle λ, as illustrated in the middle of Figure 1. Their coordinates are as follows:

$$A^m_+ = (R\cos\lambda, R\sin\lambda, \ \ \mathcal{H}(\lambda)), \qquad A^n_- = (R\cos\lambda, R\sin\lambda, -\mathcal{H}(\lambda)), \tag{1}$$

with $\lambda \in (\lambda_i, \lambda_e)$, and $\mathcal{H}(\lambda) = H + 0.5\Delta H(1 + \cos(\lambda))$. Note that $\lambda_i = -\gamma_m$ and $\lambda_e = \pi + \gamma_m$ with $\gamma_m \in (0, 0.5\pi)$ as the fan-angle. The T-line connects A^i_+ and A^i_-, and thus is parallel to the z-axis. Any point on the T-line,

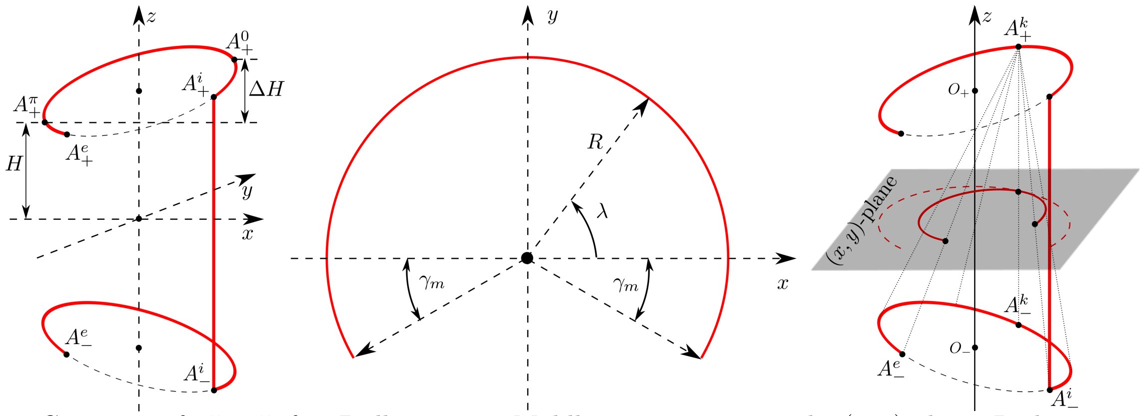

Figure 1: Geometry of ELE. Left: 3D illustration. Middle: projection onto the (x, y)-plane. Right: terminology.

A^i_h is defined as:

$$A^i_h = (R\cos\lambda_i, R\sin\lambda_i, h), \qquad h \in [-\mathcal{H}(\lambda_i), \mathcal{H}(\lambda_i)]. \tag{2}$$

Note that the ELE trajectory is periodically repeatable along the z-axis and all the curve components, i.e., EE, LE and EL, connect each other at their endpoints. This feature allows for smooth and continuous scanning.

For convenience, we define some terminology, as shown in the right of Figure 1. We call the surface, which connects A^m_+ on the upper T-arc to all the points on the lower T-arc, U-cone surface from A^m_+. The intersection between the (x, y)-plane and the U-cone from A^m_+ with polar angle λ is denoted as R-arc(λ).

3. R-LINE COVERAGE

The R-line coverage of the ELE trajectory is defined as the set of points that belong to a line connecting two points on the source trajectory. This set of points can be divided into three subsets, i.e., R-line coverage of i) Ellipse-Ellipse (EE), ii) Ellipse-Line (EL) and iii) Line-Ellipse (LE). Like Theorem 2 in [4], we have been able to prove that, for a given ROI that is centered around the z-axis, the worst R-line coverage is in the (x, y)-plane. Also, the EL and LE R-line coverage are symmetric relative to the (x, y)-plane. Therefore, we only analyze the EE and LE coverage in the (x, y)-plane, from which the complete analysis of ELE R-line coverage can be derived.

3.1 EE R-line coverage in the (x, y)-plane

The EE R-line coverage is obtained by connecting all the points on the upper T-arc to all the points on the lower T-arc. It also can be viewed as a union of all the U-cone surfaces. Let A^m_+ be a point on the upper T-arc with polar angle λ_+, and A_-^n be a point on the lower T-arc with λ_-. Then the intersection between the (x, y)-plane and the line that connects A_+^m and A_-^n, has the x and y coordinates as below:

$$\begin{cases} \dfrac{x}{R} & = \dfrac{\cos\alpha\cos\beta + d(\cos^2\alpha - \sin^2\beta)}{1 + d\cos\alpha\cos\beta} \\ \dfrac{y}{R} & = \dfrac{\sin\alpha\cos\beta + d\sin\alpha\cos\alpha}{1 + d\cos\alpha\cos\beta}, \end{cases} \tag{3}$$

where: $\alpha = 0.5(\lambda_+ + \lambda_-)$, $\beta = 0.5(\lambda_+ - \lambda_-)$ and $d = 0.5\Delta H/(H + 0.5\Delta H)$, with $\lambda_{+,-} \in [\lambda_i, \lambda_e]$. For a fixed λ_+, the cancellation of λ_- yields an equation of ellipse, which actually is the expression of R-arc(λ_+). This observation indicates that the EE R-line coverage is a union of all the R-arcs with λ_+ varying from λ_i to λ_e. Two examples with coarse samples in λ_+ can be found in Figure 2(a) and (b). In practice, (x, y) is usually

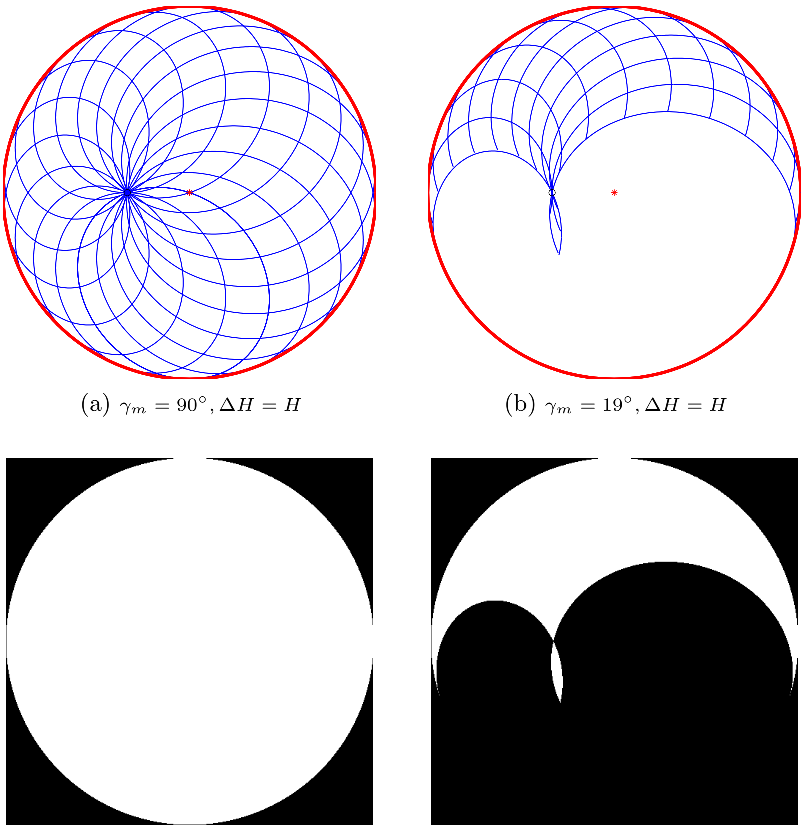

(a) $\gamma_m = 90°, \Delta H = H$ (b) $\gamma_m = 19°, \Delta H = H$

(c) $\gamma_m = 90°, \Delta H = H$ (d) $\gamma_m = 19°, \Delta H = H$

Figure 2: R-line coverage of the EE trajectory. (a) and (b): numerical simulations with a coarse sampling in λ_+. (c) and (d): analytical simulations with white as the coverage.

given and we would like to know whether there is an R-line going through this point or not. This problem can be solved by inverting Equation 3. We have been able to obtain an analytical solution of this problem. This solution then allows quick calculation of R-line coverage for a given (x, y) in the (x, y)-plane. The above solution was used to obtain Figures 2(c) and (d), in which the white areas represent the R-line coverage.

A careful analysis allowed us to identify the following properties, which are identified in Figure 3. First, all the R-arcs are tangent to the cylinder surface, $\mathcal{S}$. For example, in Figure 3(a), the R-arc(λ_+), which belongs to the U-cone from A_+^k, is tangent to the projection of A_+^k onto the (x, y)-plane, $A_)^k$, as shown in Figures 3(a) and (b). Second, the center and orientation of each R-arc can easily found. Let A_-^π and A_-^0 be points on the lower T-arc with polar angles π and 0, respectively. The lines $A_+^k A_-^\pi$ and $A_+^k A_-^0$ intersect with the (x, y)-plane at E and F, respectively. Then, the middle point of line segment EF, O_k, is the center of R-arc(λ_+), as shown in Figure 3(b). The major axis of R-arc(λ_+) lies on $\mathcal{L}$, which is parallel to the line connecting A_0^k and A_-^π and goes through O_k. This indicates that the angle between x-axis and $\mathcal{L}$ is $0.5\lambda_+$. Finally, note that all the R-arcs

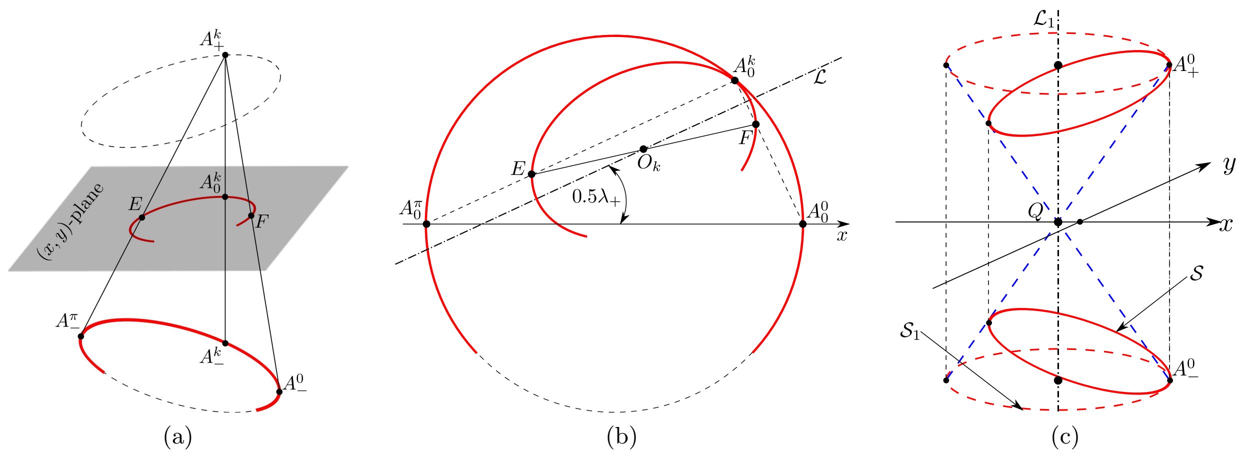

Figure 3: (a) 3D illustration of R-arc(λ_+). (b) Properties of R-arc(λ_+). (3) Geometric meaning of the common point of all the R-arcs in the (x, y)-plane.

in Figure 2(a) intersect at a common point, we call it critical point Q. This observation can be validated by Equation 3, in which, $(x, y) = (-Rd, 0)$ if $\cos\beta = -d\cos\alpha$. It means, for a full scan, picking any point on the upper T-ellipse, there always exists a point on the lower T-ellipse, such that the line connecting both points goes through the critical point $Q : (-Rd, 0)$. Figure 3(c) illustrates the geometric meaning of Q. The circular cylinder surface $\mathcal{S}$ is inscribed to another cylinder surface $\mathcal{S}_1$ along the line connecting A_+^0 and A_-^0, and Q lies on the symmetry axis of $\mathcal{S}_1$. There exist two ellipses (dashed red), such that they go through A_+^0 and A_-^0. By construction, we obtain a pair of cones (dashed blue) that shares Q as their vertex point. Now the T-arcs can be found viewed as the intersections between this pair of cones and two planes. Those two planes are orthogonal to the (x, z)-plane and intersect along a line of equation: $x = c$ with $c < -R$.

3.2 LE and ELE R-line coverage in the (x, y)-plane

The R-line coverage of the LE trajectory can be acquired by connecting all the points on the T-line to all the points on the lower T-arc. More intuitively, the coverage is the volume bounded by the U-cone surface from A_+^i and the plane defined by A_+^i, A_-^i and A_-^e. Therefore, in the (x, y)-plane, the R-line coverage of the LE trajectory is an area within R-arc(λ_i). An analytical simulation result is shown in the left of Figure 4. By adding the coverage of the EE, LE trajectories in the (x, y)-plane, we are now able to obtain the R-line coverage of the ELE trajectory in the (x, y)-plane. A simulation result is given in Figure 4 (right).

4. ROI R-LINE COVERAGE

According to Section 3.1, the R-arcs in the (x, y)-plane intersect at the critical point Q, as shown in Figure 5(a). Also note from Figures 2(a) and (b) that Q is the intersection of R-arc(λ_i) and R-arc(λ_e), which delimite the EE R-line coverage in the (x, y)-plane. As long as $\lambda_e - \lambda_i < 2\pi$, there always exists an area in the neighbor of Q that is not covered by R-lines. Therefore, for a cylindrical ROI that is centered on the z-axis, the biggest admissible radius is $r = Rd$, as shown in Figure 5(a) and (b).

However, in practice, we usually first have the radius r, upon which we need to choose ΔH. A short scan has been chosen with the fan-angle: $\gamma_m = \arcsin r/R$. According to the previous paragraph, we get ΔH by simply

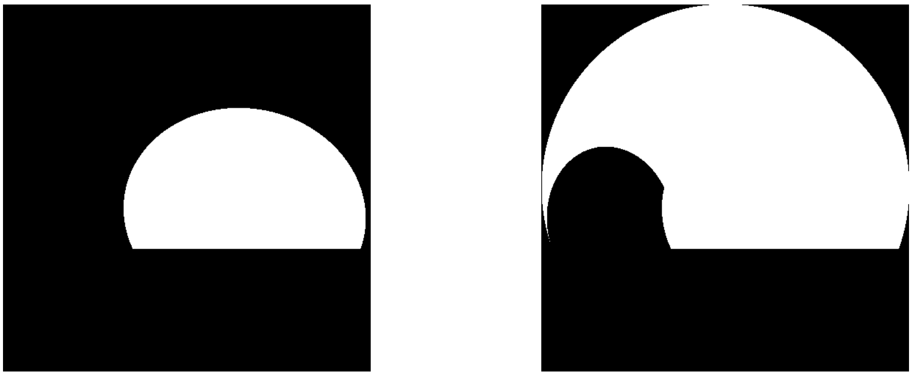

Figure 4: LE (left) and ELE (right) R-line coverage (white) with $\gamma_m = 19°$ and $\Delta H = H$.

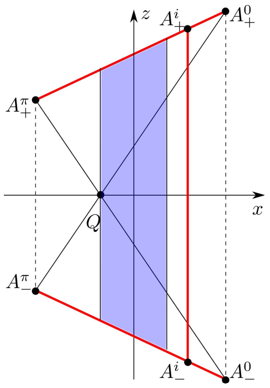

(a)

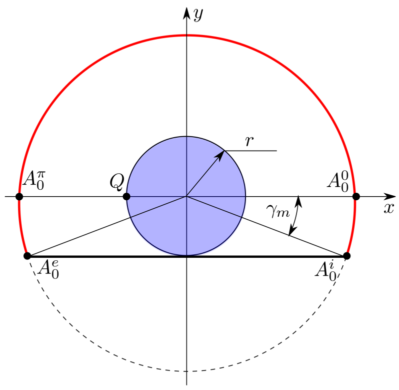

(b)

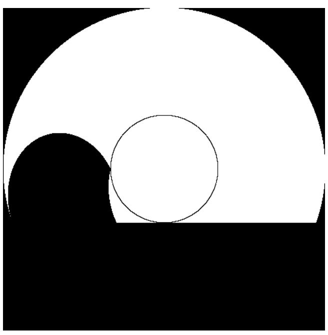

(c) $r = R/3$, $\Delta H = H$

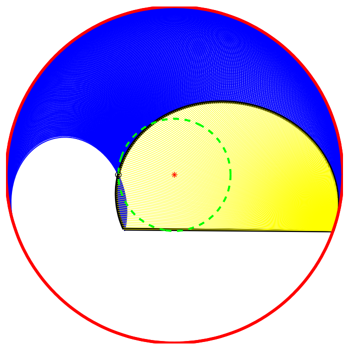

(d) $r = R/3$, $\Delta H = H$

Figure 5: Illstration of the ROI design. (a) The projection of the ELE Trajectory onto the (x, z)-plane. (b) The projection onto the (x, y)-plane. (c) Analytical simulation: the black circle stands for the ROI. (d) Numerical simulation: blue for the coverage of EE, yellow for the coverage of LE and dashed green line for the ROI.

inverting the expression of d, and get:

$$\Delta H = 2Hr/(R - r). \tag{4}$$

We were able to prove that, for a short scan with a given radius of ROI $r < 0.7R$, the choice on ΔH using Equation 4 can guarantee sufficient R-line coverage within the ROI. An example with both analytical and numerical simulations are illustrated in Figure 5(c) and (d). Both figures show that the R-line coverage within the ROI (black circle in (c) and green dashed circle in (d)) is sufficient.

5. CONCLUSION

We have presented a new trajectory, i.e., Ellipse-Line-Ellipse, which allows a smooth and continuous scanning. We have been able to show that it is periodically repeatable along the z-axis and can be designed such that the R-line coverage within a typical ROI is sufficient.

ACKNOWLEDGMENTS

This work was partially supported by a grant from Siemens AG, Healthcare Sector and by the US National Institutes of Health (NIH) under grant R21 EB009168. The concepts presented in this paper are based on research and are not commercially available. Its contents are solely the responsibility of the authors and do not necessarily represent the official views of the NIH.

REFERENCES

[1] Katsevich, A. I., "An improved exact filtered backprojection algorithm for spiral computed tomography," *Adv. Appl. Math* **32**, 681–697 (May 2004).

[2] Pack, J. and Noo, F., "Cone-beam reconstruction using 1d filtering along the projection of m-lines," *Inverse Problems* **21**, 1105–1120 (April 2005).

[3] Zou, Y. and Pan, X., "Exact image reconstruction on pi-lines from minimum data in helical cone-beam ct," *Phys. Med. Biol.* **49**, 941–959 (Feb 2004).

[4] Yu, Z., Wunderlich, A., Dennerlein, F., Lauritsch, G., and Noo, F., "Line plus arc source trajectories and their r-line coverage for long-object cone-beam imaging with a c-arm system," *Phys. Med. Biol.* **56**, 3447–71 (May 2011).